International Journal Of Engineering Research And Development
e- ISSN: 2278-067X, p-ISSN: 2278-800X, www.ijerd.com
Volume 20, Issue 8 (August, 2024), PP. 220-228

Sensing of Divalent Zinc with a Simple Ratiometric-Fluorescent Sensor

Ibrahim Uyanik[1,*], Arwa Alsaleh[2]
[1]*Department of Metallurgical and Materials Engineering, Faculty of Technology, Selcuk University, 42075 Konya, Turkey, https://orcid.org/0000-0002-1028-8293*
[2]*Department of Chemistry, Faculty of Science, Selcuk University, 42031 Konya, Turkey, https://orcid.org/0000-0002-0587-3228*
[*]*Corresponding Author: ibrhm.uyanik@gmail.com*

ABSTRACT-*In this this study, the sensing capabilities of the probe 2-[2-(1H-imidazol-5-yl)vinyl]-1-ethylquinolin-1-ium iodide (QIM) were evaluated using a variety of metal cations (Li^+, Na^+, K^+, Rb^+, Cs^+,Mg^{2+}, Ba^{2+}, Ca^{2+}, Sr^{2+}, Mn^{2+}, Fe^{3+}, Co^{2+}, Ni^{2+}, Cu^{2+}, Ag^+, Zn^{2+}, Cd^{2+}, and Pb^{2+}) in the solution phase of acetonitrile (MeCN) using fluorescence and absorption spectroscopy. The probe exhibited distinct and selective responses to Zn^{2+} ions in MeCN. It demonstrated outstanding selectivity for Zn^{2+} over other cations, exhibiting enhanced fluorescence and a red-shifted emission from 377 nm to 415 nm. The fluorescence ratio $I_{415\ nm}/I_{377\ nm}$ showed a strong linear correlation with Zn^{2+} concentrations from 0 μM to 10 μM, enabling effective ratiometric Zn^{2+} ion detection: the detection limit of the probe for Zn^{2+} was determined to be 1.47 μM in MeCN. Further, the binding mechanism of the sensor for detecting Zn^{2+} ions was investigated through Job's plot analysis, and Benesi-Hildebrand study. Job's plots revealed that the probe formed complexes with Zn^{2+} in the ratio of 1:1. Moreover, the binding constant for the probe-Zn^{2+} complex was determined to be 4.48×10^4 M^{-1} by Benesi-Hildebrand equations.*

Keywords: *fluorescence, ratiometric sensing, enhanced fluorescence, divalent zinc, chemosensor*

Date of Submission: 10-08-2024 Date of Acceptance: 21-08-2024

I. INTRODUCTION

Due to the importance of different anions, cations and neutral molecules in various processes such as medicinal chemistry, environmental monitoring, and industrial applications, the recognition of these species has fascinated the scientific community for many years, leading to the development of various molecular sensors. Divalent zinc (Zn^{2+}) is especially important during periods of rapid growth, such as infancy, childhood, and adolescence. Zinc deficiency can have detrimental effects on physical and cognitive development, leading to stunted growth, impaired learning, and increased susceptibility to infections [1–5]. The increased level of zinc can lead to a range of harmful effects on the nervous system, causing several neurological conditions like Alzheimer's disease [6], Parkinson's disease [7], hypoxia ischemia [8], and epilepsy [9]. Zinc also plays a crucial role in various industrial applications, including the production of alloys such as brass, Ni-Ag, and steel. Additionally, zinc is utilized in the manufacturing of various materials and products like rubbers, batteries, electrical equipment, and pharmaceuticals [10, 11]. Its ability to protect steel products from oxidation and corrosion is attributed to its higher oxidation potential compared to iron [12]. Considering the importance of Zn^{2+} in various scientific disciplines, including materials science, environmental monitoring, and analytical chemistry, the development of accurate and reliable identification and quantification methods for Zn^{2+} sensing in various materials is crucial.

Traditional methods for Zn^{2+} detection, such as atomic absorption spectrometry [13], capillary electrophoresis [14], ICP-MS [15], and ion chromatography [16] often require specialized equipment and time-consuming sample preparation steps [17]. However, the development of chemosensors offers a simpler and more cost-effective alternative for the detection of different ions, with the added advantage of real-time monitoring capabilities [18–20]. Further, fluorescent chemosensors, in particular, have gained significant attention in recent years due to their ability to selectively and sensitively detect and quantify specific target analytes, including heavy metal ions such as Zn^{2+}. They typically consist of a fluorophore, which serves as the signal emitter, and a receptor moiety that can be designed to selectively bind to a particular analyte through various interactions such as hydrogen bonding, electrostatic interactions, or specific molecular recognition, leading to a change in the fluorescence properties of the sensor. Thus, these sensors can be categorized into different groups based on their signaling process: turn-off, turn-on, and ratiometric. Turn-off sensors have

quenched fluorescence, turn-on sensors have enhanced fluorescence, and ratiometric sensors have shifted fluorescence upon recognition of the target analyte, with a generally reversible process [21–23]. Despite the development of numerous fluorescent sensors using different fluorophores for detecting zinc ions, there is still a need for new Zn^{+2}-selective fluorescent sensors with high affinity and selectivity over other relevant metal ions. Currently, the development of a single receptor that can recognize metal ions ratiometrically is an area of growing interest among researchers. Therefore, one of the important strategies to address this challenge is to utilize a ratiometric fluorescent sensor design, where the sensor emits different wavelengths of light depending on whether it is bound to Zn^{+2} or other cations. This can provide a more reliable way to distinguish between the two metal ions, as their binding to the sensor would result in distinct fluorescent signals.

In our previous study[24], we synthesized the cationic probe QIM containing quinaldinium and imidazole derivatives and evaluated its fluorescence sensor properties against some anions. The specific coordination pattern of the receptor is essential for host-guest chemistry. Therefore, the careful selection of a receptor that can effectively and preferentially bind to a cation is crucial for achieving improved selective detection. Imidazole derivatives have shown great potential as sensors for metal ions due to their exceptional fluorogenic and chromogenic properties [25–30]. These properties allow imidazole derivatives to undergo color changes or fluorescence emission in the presence of specific metal ions, making them useful for detecting and quantifying metal ions in various samples. Ultimately, taking into account all these considerations, in this current study, the fluorescence sensor properties of the probe QIM against some metal ions were investigated and it was revealed that the probe QIM specifically showed ratiometric sensor properties capable of detecting divalent zinc cation.

II. MATERIAL AND METHODS

Materials and Instruments

^{1}H NMR spectra were obtained in DMSO-d_6 on a Bruker 400 MHz spectrometer. FT-IR spectra data were recorded with a Brucker Vector 22 FT-IR spectrometer. Absorbance changes were recorded using a Perkin Elmer Lambda-35 UV-visible double beam spectrophotometer with standard 1.00 cm quartz cells at room temperature. Fluorescence emission and excitation spectra were recorded on a PerkinElmer LS 55 spectrometer. Pre-coated silica gel plates (SiO_2, Merck PF254) were used for analytical TLC analyses. All reagents, chemicals, and solvents used in the experiments were sourced from commercial suppliers and utilized without further purification, unless otherwise specified.

General Procedure of Spectroscopic Studies

A stock solution of QIM at a concentration of 1.0 mM was prepared in MeCN. Additionally, stock solutions of metal ions at a concentration of 1.0 mM were prepared in MCN by using their perchlorate salts. For fluorescence and absorbance spectra, test solutions were prepared by adding 30 µL of QIM into a test tube, followed by the addition of an appropriate aliquot of each metal stock solution, and then diluting the solution to a total volume of 3.0 mL. The same procedure was used for fluorescence titration and interference study involving co-existing ions in a solution containing QIM-Zn^{2+} complex. Fluorescence intensity measurements were conducted at excitation and emission wavelengths of 250 nm and 377 nm, respectively. Each measurement was repeated twice to ensure consistency, and sufficient time was allowed before recording each spectrum to ensure uniformity of the solution.

III. RESULTS AND DISCUSSION

The synthesis and characterization of the probe QIM used as the ratiometric fluorescent sensor, are given in detail in our previous paper [24]. The chemical structure of QIM is shown in Figure 1.

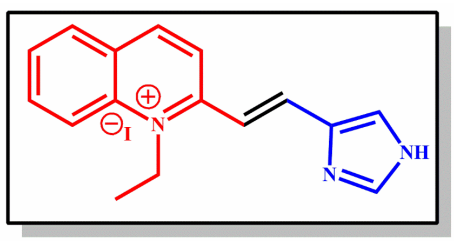

QIM

Figure1: The probe QIM: 2-[2-(1H-imidazol-5-yl)vinyl]-1-ethylquinolin-1-ium iodide [24]

3.1 Cation Sensing Ability of QIM: Fluorescence and UV-Vis Studies

The investigation into the cation recognition capability of QIM towards various cations (Li^+, Na^+, K^+, Rb^+, Cs^+, Mg^{2+}, Ba^{2+}, Ca^{2+}, Sr^{2+}, Mn^{2+}, Fe^{3+}, Co^{2+}, Ni^{2+}, Cu^{2+}, Ag^+, Zn^{2+}, Cd^{2+}, and Pb^{2+}) was conducted utilizing UV-

vis and fluorescence spectroscopy in MeCN. The absorption behavior exhibited by QIM did not show a significant change with the addition of other cations except for zinc, as can also be seen in Fig. 2a. However, with the addition of zinc, although the intensity of the maximal absorbance of QIM decreased, a new red-shifted absorption peak emerged at a wavelength of 370 nm. The emergence of the new absorption band was attributed to the formation of the QIM-Zn complex, indicating that QIM exhibits a high selectivity towards Zn^{2+} compared to other competitive cations. Similarly, the fluorescence behavior of QIM towards aforementioned metal ions was systematically examined under uniform experimental conditions. The fluorescence emission profile of free QIM (10 µM) in MeCN displayed a peak emission at 377 nm (with an excitation wavelength of 250 nm), as illustrated in Fig. 2b. The introduction of aforementioned cations (100 µM) other than Zn^{2+} into the QIM solution resulted in varying degrees of quenching effects on the fluorescence emission of QIM. Notably, metal ions such as Fe^{3+} and Cu^{2+} lead to almost complete quenching of QIM emission, accompanied by the emergence of a new emission band with very low intensity centered at 450 nm. However, a distinct scenario unfolds upon the addition of Zn^{2+}. Specifically, upon the introduction of Zn^{2+} into the QIM solution, a significant decrease in fluorescence intensity at 377 nm was observed, yet accompanied by a red shift in the emission band to 415 nm. The results indicate that only Zn^{2+} elicits a significant red shifted intensity enhancement in the emission spectrum of QIM, underscoring its superior selectivity compared to other metal ions. A red shift similar to divalent zinc was also observed for Cd^{2+}, but in this case a decrease in fluorescence intensity was also observed. This shows that Zn^{2+} and Cd^{2+} cations in the same environment can be separated depending on the degree of the fluorescence intensity.

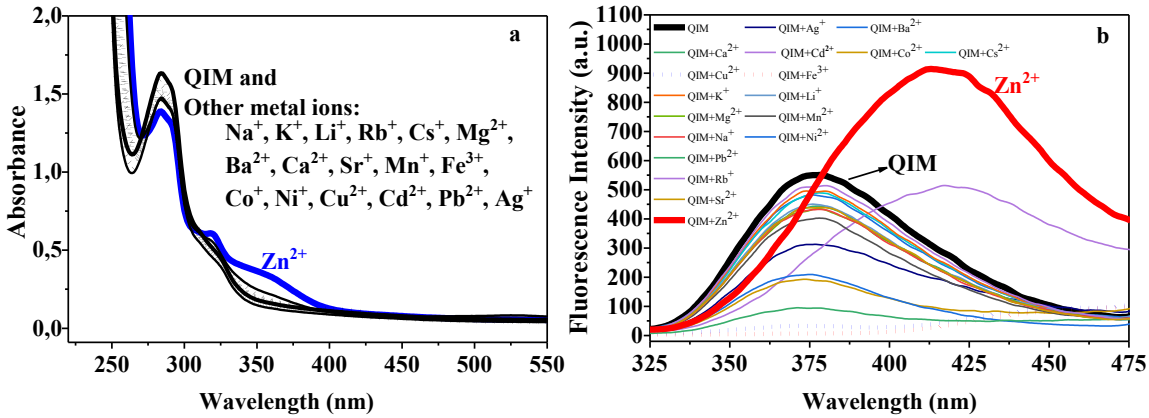

Figure2: Absorption (a) and emission (b) spectra of the probe QIM (10 µM) in the presence of different metal ions (100 µM) in MeCN solution (λ_{ex} = 250 nm)

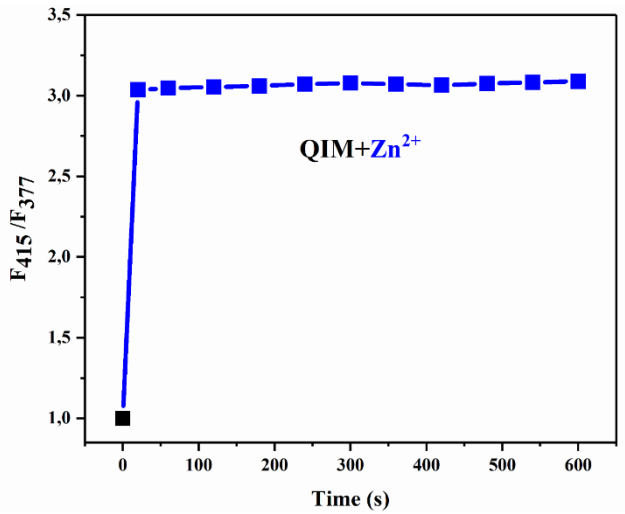

Figure3: Time-dependent fluorescence intensity ratio (F_{415}/F_{377}) of QIM (10 µM) in MeCN after the addition of 10 µM Zn^{2+}

The response time plays a crucial role in the assessment of detection methodologies. The selective responses of the QIM probe were evaluated by introducing Zn^{2+} (10 µM) into MeCN (10 µM). As depicted in Fig. 3, the fluorescence intensity ratio (F_{415}/F_{377}) stabilized at approximately 20 seconds, indicating the rapid and

efficient response of the probe to Zn^{2+}, rendering it suitable for the swift detection of Zn^{2+} in MeCN. A crucial aspect of excellent chemosensors is their high selectivity. The evaluation of QIM's selectivity towards Zn^{2+} ions and its interaction with other metal ions was conducted through fluorescence assessments. Thus, the potential interference of various metal ions on the sensing mechanism was thoroughly investigated. As shown in Fig. 4, results showed that only the addition of Zn^{2+} elicited clear ratiometric responses. Further, even in the presence of equimolar concentrations of other metal cations (100 μM), a similar degree of ratiometric fluorescence was observed, confirming the robust anti-interference capability of the Zn^{2+} sensor.

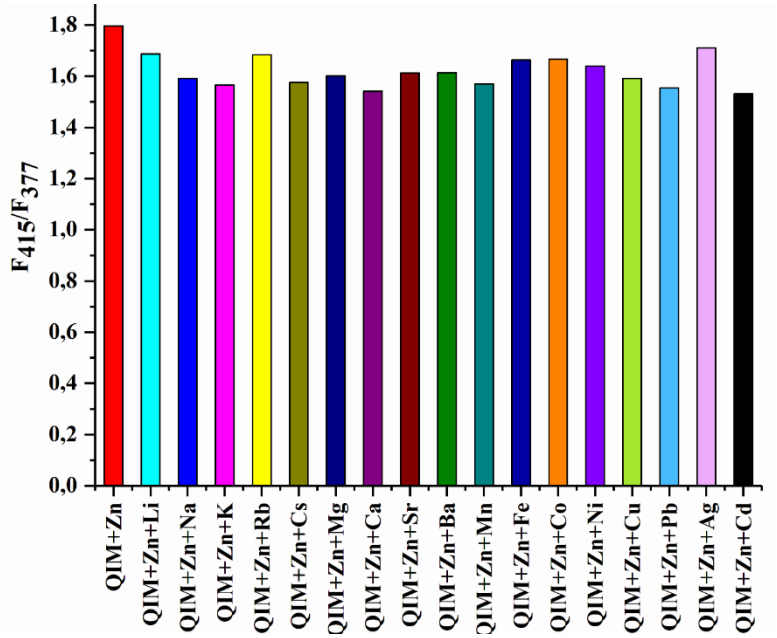

Figure4: Ratiometric fluorescence of the QIM-Zn in the absence and presence of the other metal ions

3.2 Fluorescence Titration Studies for Zn^{2+} Sensing: Calibration Curve, Limit of Detection, and Stoichiometry

The fluorescence titration experiments in MeCN were performed to study QIM's sensing abilities further towards Zn^{2+}.

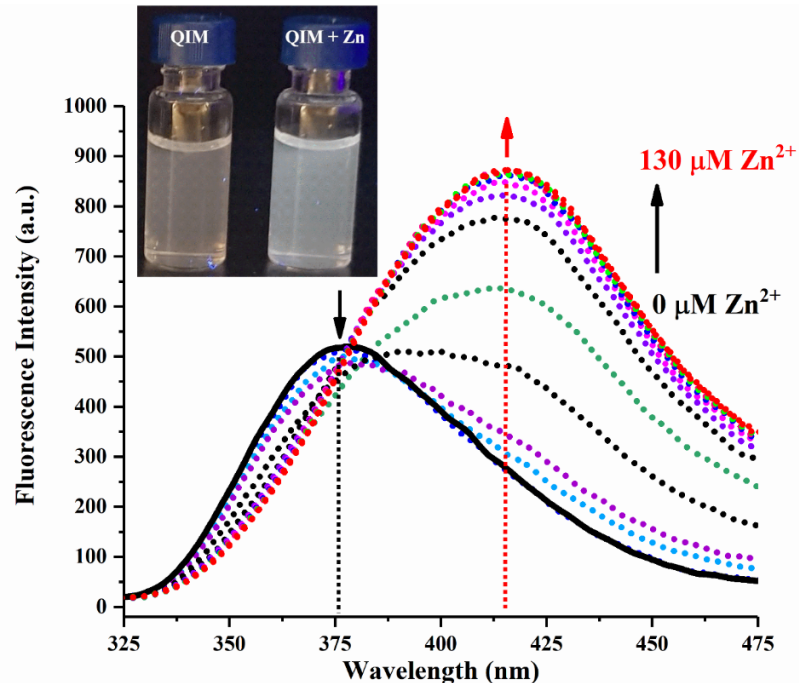

Figure5: Fluorescence intensity changes of the probe QIM (10 µM) in the presence of an increasing concentration of Zn^{2+} in MeCN (λ_{ex}= 250 nm). Photographs taken under a UV lamp

The results, depicted in Fig. 5, indicated that QIM could function as a ratiometric sensor for Zn^{2+}. As Zn^{2+} (0.0–130 µM) was gradually added to a QIM solution (10 µM), the emission peak at 377 nm decreased while a new peak at 415 nm emerged. Further addition of Zn^{2+} (0.0–13.0 equiv.) revealed a clear ratiometric change in fluorescence spectra, confirming the formation of a QIM-Zn^{2+} complex. An increase of approximately twofold in the fluorescence intensity at a wavelength of 415 nm, in comparison to the emission intensity exhibited by free probe QIM at 375 nm, was observed until reaching a saturation point following the introduction of 1.0 equivalent of Zn^{2+} (refer to Fig. 6). Subsequently, the fluorescence intensity at 415 nm appeared to reach a plateau, showing minimal variation upon the addition of Zn^{2+} beyond the 1.0 equivalent mark. Further increments in the amount of Zn^{2+} did not result in a discernible enhancement in the emission band intensity of the QIM sensor at 415 nm. Moreover, a noticeable enhancement in the fluorescence intensity ratio (F_{415nm}/F_{377nm}) is evident, transitioning from 0.4 to 1.5 as depicted in Fig. 6. The ratios of intensity at 415 and 377 nm (F_{415nm}/F_{377nm}) exhibit a progressive increase up to the introduction of 1 equivalent Zn^{2+}. The saturation in the fluorescence enhancement at a low concentration of Zn^{2+} suggests that the binding sites of QIM are nearly all occupied by Zn^{2+}. This indicates a strong affinity between QIM and Zn^{2+}. Furthermore, when Zn^{2+} ions are added to the QIM solution in MeCN and exposed to UV light, a blue fluorescence is observed. This blue fluorescence serves as a clear indication of the colorimetric sensing capability of QIM towards Zn^{2+} (Fig. 5 inset).

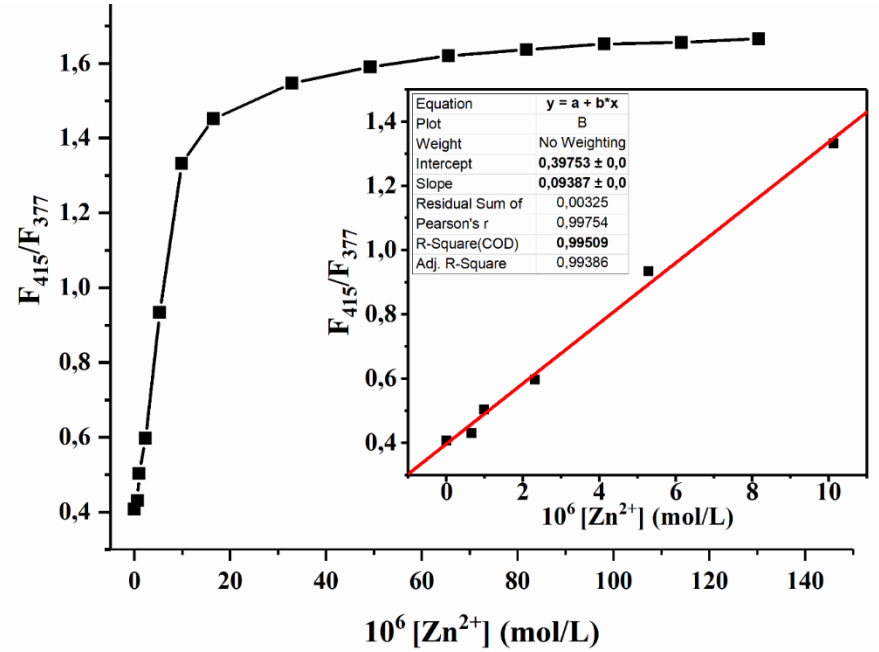

Figure 6: Fluorescence ratiometric plot constructed from the intensities of the bands at 377 nm and 415 nm for QIM (10 µM) upon addition of Zn^{2+} with different concentrations (0–130 µM). The inset is the linearity of F_{415}/F_{377} to Zn^{2+} ion concentration and shows how the ratio of the intensities at 415 nm and 377 nm changes linearly with the concentration of Zn^{2+}

From the fluorescence titration data, a strong linear correlation between the fluorescence intensity ratios and Zn^{2+} concentrations within the range of 0 µM to 10 µM with a correlation coefficient of 0.9951 is established (Fig. 6 inset). According to this ratiometric calibration curve, the limit of detection was calculated to be 1.47 µM by the equation below.

(1)

where *sb* is the standard deviation of the blank solution and *k* is the slope of the calibration curve. The stoichiometric composition of the QIM-Zn^{2+} complex was validated using Job's method, also known as the method of continuous variations. For this purpose, the solutions of equimolar concentration (1.5×10^{-5} M) of the two components are mixed in different ratios varying from 1:9 to 9:1. The outcomes of the Job's plot experiments utilizing both fluorescence and absorption spectroscopy techniques to ascertain the stoichiometry between QIM and Zn^{2+} suggest that a 1:1 binding mode exists between QIM and Zn^{2+} ions (Fig. 7).The association constant (Ka) of the QIM-Zn complex was determined by graphically plotting $1/F_0$-F against $1/[Zn^{2+}]$

[31–33]. where, in the absence and presence of various concentrations of Zn^{2+}, the fluorescence intensities of QIM are denoted by F_0 and F, respectively Through linear fitting of the data to the Benesi-Hildebrand equation, the Ka value was calculated to be 4.48×10^4 M^{-1}, as illustrated in Fig. 8. The linear relationship observed in the plot provides additional evidence supporting the formation of a 1:1 complex between QIM and Zn^{2+}.

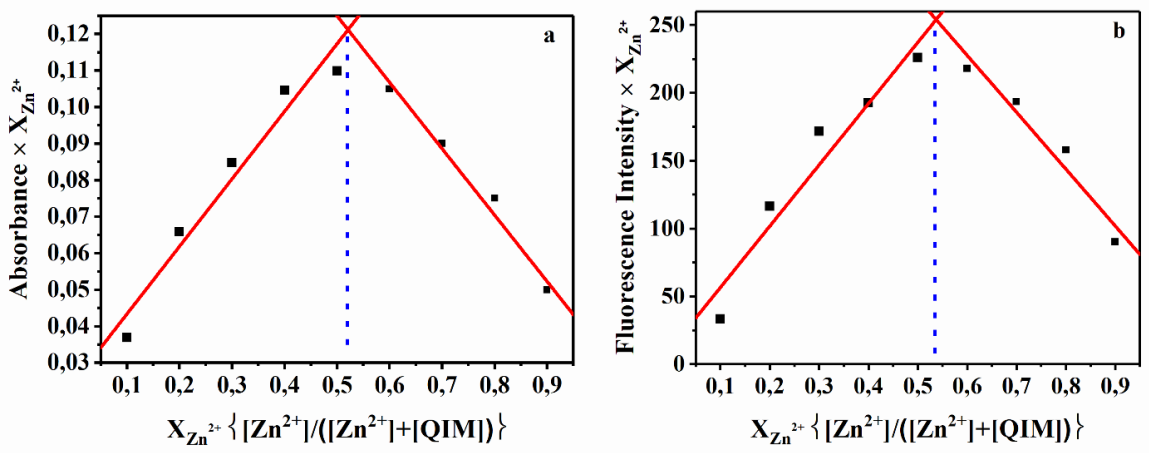

Figure 7: Job's plot for determining the binding stoichiometry of the probe QIM with Zn^{2+} in MeCN solution from (a) UV-vis spectral studies and (b) Fluorometric studies. The total concentration of QIM and Zn^{2+} is 100 µM, monitored at the wavelength of 415 nm

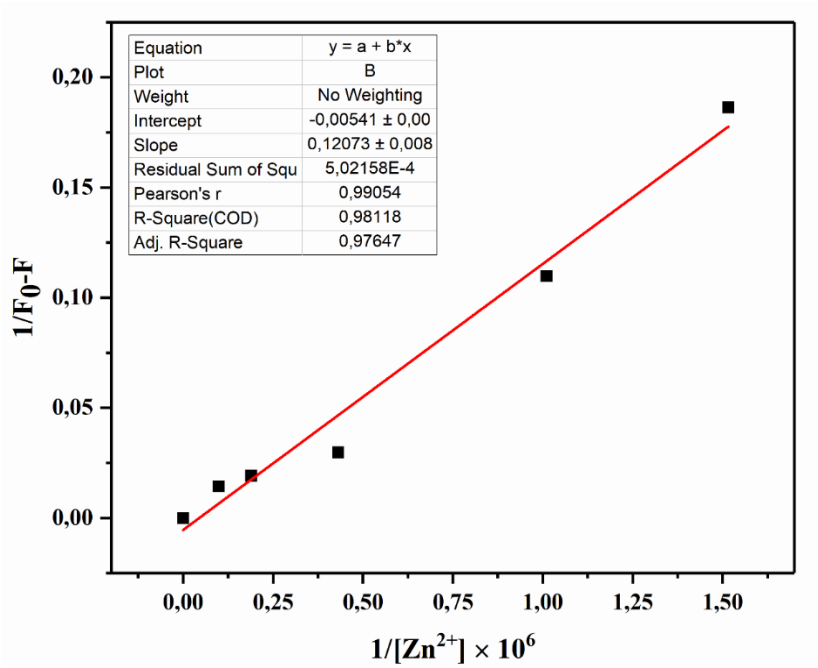

Figure 8: Benesi-Hildebrand curve from the fluorescence data for determining the binding affinity between QIM (10 µM) and Zn^{2+}

3.3 FT-IR and ^{1}H NMR studies

The coordination of QIM with Zn^{2+} was confirmed through FT-IR spectroscopy. Upon systematic analysis of the FT-IR spectrum of QIM (Fig. 9), distinct bands (cm^{-1}) were observed at 3417 (N-H), 3057 for aromatic (C-H), 1595 for (C=C), 1348 for aromatic (C-N), and 1150 for (C-N). A comparison of the FT-IR spectra of QIM before and after the addition of Zn^{2+} revealed shifts in certain IR peaks. Specifically, the aromatic C-N stretching peak of imidazole at 1150 cm^{-1} and the C=N-C=C stretching band of the imidazole ring at 1594 cm^{-1} were altered upon the addition of Zn^{2+}, signifying the participation of C-N and C-H functionalities in the complexation process between QIM and Zn^{2+}. Furthermore, the peak corresponding to the aromatic C-N stretching band at 1348 cm^{-1} disappeared after the complexation of QIM with Zn^{2+}. To further investigate the binding mechanism of the QIM probe, the ^{1}H NMR spectra of QIM before and after the addition of Zn^{2+} were

compared (Fig. 10). Upon complexation of QIM with Zn^{2+}, the proton peak of the imidazole moiety shifted to a lower field due to the reduction of electron density following complexation with Zn^{2+}. The observed downfield shifts are primarily attributed to N-Zn^{2+} interaction, leading to electron transfer from the N atoms to the Zn^{2+}. It is notable that the nitrogen atom of the imidazole ring, rather than N(H), interacts with the Zn^{2+} ions because the unshared electron pair of N(H) participates in cyclic conjugation, as described in the literature [33], thereby reducing the electron density of this particular N atom.

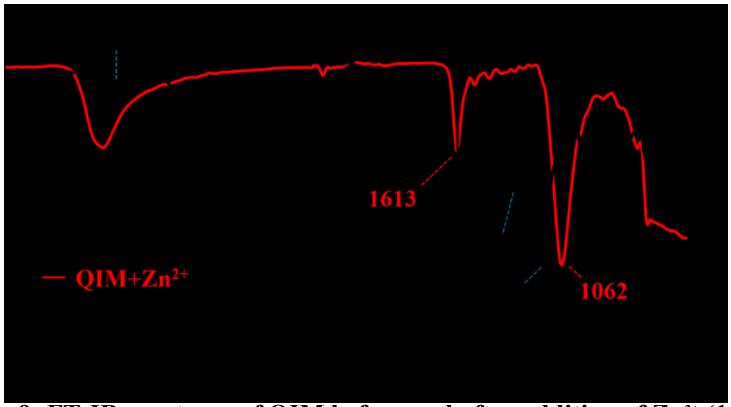

Figure 9: FT-IR spectrum of QIM before and after addition of Zn^{2+} (1 eqv.)

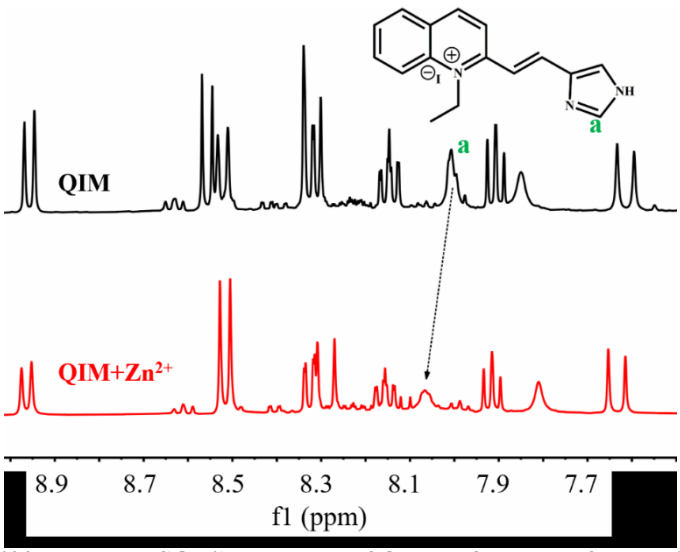

Figure 10: ^{1}H-NMR (400 MHz, DMSO-d_6) spectrum of QIM before and after addition of Zn^{+2} (1 equiv.)

3.4 Sensing Mechanism

The design of QIM incorporates a quinolinium moiety serving as a fluorophore, linked to an imidazole scaffold. The nitrogen atoms within the imidazole structure, along with the C=C double bond in QIM, are postulated to function as receptor units capable of binding with Zn^{2+} ions (Fig. 11).

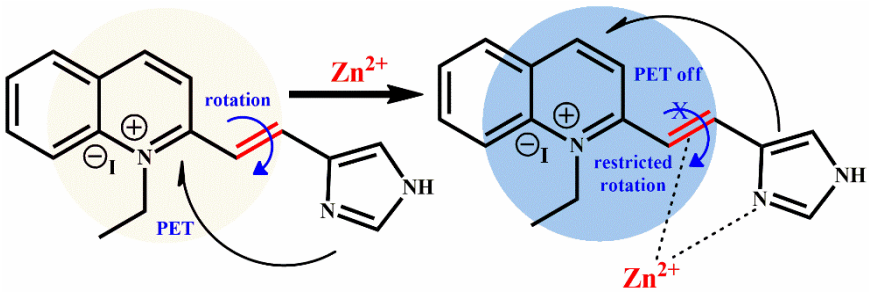

Figure 11: Schematic representation of the proposed interaction mechanism between the probe QIM and Zn^{2+} ion

Upon examination of the fluorescence spectrum of QIM at a concentration of 10 μM, a discernible single emission band at approximately 377 nm is observed under ambient conditions. This emission pattern may be attributed to an intramolecular photoinduced electron transfer (PET) process, as well as the unrestricted rotations around the C=C double bond linking the quinolinium and imidazole units. However, it can be suggested that binding of Zn^{2+} ions to the QIM probe may cause an increase in the fluorescence emission intensity by restricting the C=C double bond rotation between the quinolinium and imidazole components and blocking the effective PET process from the receptor to the fluorophore [33]. Another important point that occurs with the addition of Zn^{2+} is the red shift. In this case it can be said that the covalent linkage between quinolinium with imidazole can form a π-electron conjugation system with electron-rich and electron-poor terminals of QIM. Thus, the interaction between the receptor and Zn^{2+} would further strengthen the push-pull effects, reflecting a redshifted emission from the fluorophore part. This is the strategy that has been successfully applied to quinoline-based ratiometric molecular probes for Zn^{2+} [34].

IV. CONCLUSION

In conclusion, the probe QIM based on quinolinium and imidazole moieties, specifically 2-(2-(1H-imidazol-5-yl)vinyl)-1-ethylquinolin-1-ium iodide, was successfully used as a ratiometric fluorescent sensor. Upon the introduction of Zn^{2+} salts into the MeCN solution of QIM, substantial alterations were observed in both its absorption and emission spectra. Specifically, the addition of Zn^{2+} resulted in increased fluorescence intensity and a shift towards longer wavelengths. This indicates that QIM can effectively detect Zn^{2+} in a selective and sensitive manner, making it a valuable ratiometric sensor for distinguishing Zn^{2+} from other competing metal ions. Lastly, we hope that the sensor's ability to detect and determine Zn^{2+} through fluorescence changes will make it a promising candidate for analytical and biological applications.

ACKNOWLEDGMENT

IU and AA express their gratitude to the Chemistry Department, Selcuk University, Türkiye for using their facilities to conduct the research analyses.

REFERENCES

[1]. Bettger, W.J., O'Dell B.L. 1981. A critical physiological role of zinc in the structure and function of biomembranes, *Life Sci*., 28:13, 1425–1438. https://doi.org/10.1016/0024-3205(81)90374-X

[2]. Prasad, A.S.1996. Zinc deficiency in women, infants and children, *J. Am. Coll. Nutr*., 15:2, 113–120. https://doi.org/10.1080/07315724.1996.10718575

[3]. Haase, H., Rink, L. 2009. The immune system and the impact of zinc during aging. *Immun. Ageing*., 6, 9. https://doi.org/10.1186/1742-4933-6-9

[4]. Prasad, A.S. 2013. Discovery of human zinc deficiency: its impact on human health and disease. *Adv. Nutr*., 4:2, 176–190. https://doi.org/10.3945/an.112.003210

[5]. Bartzatt, R. 2017. Neurological impact of zinc excess and deficiency in vivo, *Eur. J. Nutr. Food. Sf*., 7:3, 155–160. https://doi.org/10.9734/EJNFS/2017/35783

[6]. Bush, A.I. 2003. The metallobiology of Alzheimer's disease, *Trends Neurosci*., 26:4, 207–214. https://doi.org/10.1016/S0166-2236(03)00067-5

[7]. Wojtunik-Kulesza K., Oniszczuk, A., Waksmundzka-Hajnos, M. 2019. An attempt to elucidate the role of iron and zinc ions in development of alzheimer's and parkinson's diseases, *Biomed Pharmacother*, 111, 1277–1289. https://doi.org/10.1016/j.biopha.2018.12.140

[8]. Koh, J-Y., Suh, S.W., Gwag, B.J., He, Y.Y., Hsu, C.Y., Choi, D.W. 1996. The role of zinc in selective neuronal death after transient global cerebral ischemia, *Science*, 272:5264, 1013–1016. https://doi.org/10.1126/science.272.5264.1013

[9]. Doboszewska, U., Młyniec, K., Wlaź, A., Poleszak, E., Nowak, G., Wlaź, P. 2019. Zinc signaling and epilepsy, *Pharmacol. Ther*., 193, 156–177. https://doi.org/10.1016/j.pharmthera.2018.08.013

[10]. Chourasia, J., Tohora, N., Mahato, M., Sultana, T., Ahamed, S., Maiti, A., Das, S.K. 2024. A sulfone-based fluorogenic probe for cascade detection of Zn2+ and PO43− ions, *J. Mol. Struct*., 1304, 137736. https://doi.org/10.1016/j.molstruc.2024.137736

[11]. Li, J., Yin, C., Huo, F. 2016. Development of fluorescent zinc chemosensors based on various fluorophores and their applications in zinc recognition, *Dyes Pigm*., 131, 100–133. https://doi.org/10.1016/j.dyepig.2016.03.043

[12]. Kalendová, A., Kalenda, P., Veselý, D. 2006. Comparison of the efficiency of inorganic nonmetal pigments with zinc powder in anticorrosion paints, *Prog. Org. Coat*., 57:1,1–10. https://doi.org/10.1016/j.porgcoat.2006.05.015

[13]. Li, Q., Zhao, X., Lv, Q., Liu, G., 2007. The determination of zinc in water by flame atomic absorption spectrometry after its separation and preconcentration by malachite green loaded microcrystalline triphenylmethane, *Sep. Purif. Technol*., 55:1, 76–81. https://doi.org/10.1016/j.seppur.2006.11.001

[14]. Qu, F., Lin, J.M., Chen, Z., 2004. Simultaneous separation of nine metal ions and ammonium with nonaqueous capillary electrophoresis, *J. Chromatogr. A*, 1022:1-2, 217–221. https://doi.org/10.1016/j.chroma.2003.09.039

[15]. Fernández-Menéndez, S., Fernández-Sánchez, M.L., Fernández-Colomer, B., de la Flor St. Remy, R.R., Coto Cotallo, G.D., Soares Freire, A., Ferreira Braz, B., Santelli, R.E., Sanz-Medel, A., 2016. Total zinc quantification by inductively coupled plasma-mass spectrometry and its speciation by size exclusion chromatography–inductively coupled plasma-mass spectrometry in human milk and commercial formulas: Importance in infant nutrition, *J. Chromatogr. A*, 8, 246–254. https://doi.org/10.1016/j.chroma.2015.09.021

[16]. Gros, N., 2013. Ion chromatographic analyses of sea waters, brines and related samples, *Water*, 5: 659–676. https://doi.org/10.3390/w5020659

[17]. Karmegam, M.V., Karuppannan, S., Christopher Leslee, D.B., Subramanian. S., Gandhi, S., 2020. Phenothiazine–rhodamine-based colorimetric and fluorogenic 'turn-on' sensor for Zn2+ and bioimaging studies in live cells, *Luminescence*, 35:1, 90–97. https://doi.org/10.1002/bio.3701

[18]. Nolan, E.M., Lippard, S.J., 2008. Tools and tactics for the optical detection of mercuric ion, *Chem. Rev*., 108: 9, 3443–3480. https://doi.org/10.1021/cr068000q

[19]. Domaille, D.W., Que, E.L., Chang, C.J., 2008. Synthetic fluorescent sensors for studying the cell biology of metals, *Nat. Chem. Biol*.,4, 168–175. https://doi.org/10.1038/nchembio.69

[20]. Sun, W., Guo, S., Hu, C., Fan, J., Peng, X. 2016. Recent development of chemosensors based on cyanine platforms, *Chem. Rev*., 116:14, 7768–7817. https://doi.org/10.1021/acs.chemrev.6b00001

[21]. Kaur, P., Singh, K. 2023. Analyte detection: a decade of progress in the development of optical/fluorescent sensing probes, *Chem. Rec*., 23: 1, e202200184. https://doi.org/10.1002/tcr.202200184

[22]. Vidya, B., Sivaraman, G., Sumesh, R.V., Chellappa, D. 2016. Fluorescein based ''turn on''fluorescence detection of Zn2+ and its applications in imaging of Zn2+ in apoptotic cells, *ChemistrySelect,* 1:4024–4029. https://doi.org/10.1002/slct.201600863

[23]. Wang, J.T., Pei, Y.Y., Yan, M.Y., Li, Y.G., Yang, G.G., Qu, C.H., Li, Q.F. 2021. A fast-response turn-on quinoline-based fluorescent probe for selective and sensitive detection of zinc (II) and its application, *Microchem. J.*, 160:105776. https://doi.org/10.1016/j.microc.2020.105776

[24]. Uyanik, I., Alsaleh, A. 2024. Detection of iodide using a fluorescent chemosensor based on quinaldinium and imidazole moieties, *International Journal of Scientific Engineering and Science,* 8:8, 1–7.

[25]. Pandith, A., Uddin, N., Choi, C.H., Kim, H.S. 2017. Highly selective imidazole-appended 9,10-N,N′-diaminomethylanthracene fluorescent probe for switch-on Zn2+ detection and switch-off H2PO4− and CN− detection in 80% aqueous DMSO, and applications to sequential logic gate operations, *Sens. Actuators B Chem*., 247, 840–849. https://doi.org/10.1016/j.snb.2017.03.112

[26]. Ansari, S.N., Saini, A.K., Kumari, P., Mobin, S.M. 2019. An imidazole derivative-based chemodosimeter for Zn2+ and Cu2+ ions through "ON–OFF–ON" switching with intracellular Zn2+ detection, *Inorg. Chem. Front*., 6:3, 736–745. https://doi.org/10.1039/C8QI01127C

[27]. Liu, J., Wang, S., Li, W., Dong, Y., Wang, J., Song, Q., Zhang, C. 2020. A novel imidazole-based tri-nitrogen metal cations probe with better-selectivity in ionic radius and acting as a Zn2+ fluorescence turn-on sensor, *J. Mol. Struct*., 1222, 128909. https://doi.org/10.1016/j.molstruc.2020.128909

[28]. Wang, J.H., Liu, Y.M., Chao, J.B., Wang, H., Wang, Y., Shuang, S. 2020. A simple but efficient fluorescent sensor for ratiometric sensing of Cd2+ and bio-imaging studies, *Sens. Actuators B Chem*., 303, 127216. https://doi.org/10.1016/j.snb.2019.127216

[29]. Da Lama, A., Sestelo, J.P., Valencia, L., Esteban-Gómez, D., Sarandeses, L.A., Martínez, M.M. 2022. Synthesis and structural analysis of push-pull imidazole-triazole based fluorescent bifunctional chemosensor for Cu2+ and Fe2+ detection, *Dyes Pigm*., 205, 110539. https://doi.org/10.1016/j.dyepig.2022.110539

[30]. Krishnan, U., Manickam, S., Iyer, S.K. 2024. Turn-off fluorescence of imidazole-based sensor probe for mercury ions, *Sens. Diagn*., 3, 87–94. https://doi.org/10.1039/D3SD00146F

[31]. Jana, S., Dalapati, S., Alam, M.A., Guchhait, N. 2012. Fluorescent chemosensor for Zn(II) ion by ratiometric displacement of Cd(II) ion: A spectroscopic study and DFT calculation, *J. Photochem. Photobiol. A Chem*., 238, 7–15. https://doi.org/10.1016/j.jphotochem.2012.04.002

[32]. Aich, K., Goswami, S., Das, S., Mukhopadhyay, C.D. 2015. A new ICT and CHEF based visible light excitable fluorescent probe easily detects in vivo Zn2+, *RSC Adv*., 5, 31189–31194. https://doi.org/10.1039/c5ra03353e

[33]. Velmurugan K, Raman A, Don D, Tang L, Easwaramoorthi S, Nandhakumar R. 2015. Quinoline benzimidazole-conjugate for the highly selective detection of Zn(ii) by dual colorimetric and fluorescent turn-on responses, *RSC Adv*., 5:55, 44463–44469. https://doi.org/10.1039/C5RA04523A

[34]. Sadhu, K.K., Mizukami, S., Kikuchi, K. 2013. Zinc, Fluorescent Sensors as Molecular Probes, in *Encyclopedia of Metalloproteins*, Kretsinger, R.H., Uversky, V.N., Permyakov, E.A., Ed., New York, NY., Springer, 2523–2528. https://doi.org/10.1007/978-1-4614-1533-6_237